Journal of Science and Technology in Civil Engineering NUCE 2018. 12 (3): 44–50

SOME MICROSTRUCTURE PROPERTIES AT EARLY AGE OF ETTRINGITE BINDER BASED ON RICH $C_{12}A_7$ CALCIUM ALUMINATE CEMENT

Nguyen Ngoc Lam[a,*]

[a]*Faculty of Building Materials, National University of Civil Engineering, 55 Giai Phong road, Hai Ba Trung district, Hanoi, Vietnam*

Article history:
Received 24 January 2018, Revised 04 April 2018, Accepted 27 April 2018

Abstract

The mineral composition of calcium aluminate cements is traditionally based on CA (monocalcium aluminate - $CaO \cdot Al_2O_3$). Recently, a new cement with the main compound of $C_{12}A_7$ (Mayenite) has been developed for rapid hardening binder. This cement is used in conjunction with a sulfate binder to form a new type binder called ettringite binder due to the high quantity of ettringite in the hydration product, opened new possibilities for mortar and concrete formulations. This paper focuses on some microstructure characteristics of the ettringite binder based on a $C_{12}A_7$ rich cement and a hemihydrate at early age. Some important characteristics of this binder were found, such as: short setting time (about 40–50 minutes), rapid expansion just after initial setting time, rapid evolution of porosity and bound water during the first 5 hours of hydration. The correlation between bound water and porosity of hardened binders was also found in this paper.

Keywords: ettringite binder; early-age; setting; $C_{12}A_7$; hemihydrate.

© 2018 National University of Civil Engineering

1. Introduction

Within the last few decades, the number of bridges, roads, houses damaged or degraded has been being increased [1, 2]. Therefore, rapid hardening repair materials are in high demand for these applications as they allow for minimizing traffic delays, road closures and timesaving, etc... [2, 3]. Calcium aluminate cement (CAC), whose mineral composition is traditionally designed around monocalcium aluminate - $CaO \cdot Al_2O_3$ (CA), is a rapid hardening binder and usually used for special applications where high early strength and increased durability are desired. Their setting time is close to that of OPC, typically around 3 hours, but their hardening rate is in the range of 10 MPa to 20 MPa (compression) per hour from setting. This rapidity is compatible with applications that require compressive strength from 10 MPa to 30 MPa after 4h to 6h, such as industrial floor repairs [4–6]. For applications requiring higher rapidity, the hydration has to be accelerated. The most common way to accelerate hydration of CAC is adding lithium salts (Li_2CO_3 or Li_2SO_4 for example) [7–9]. Recently,

*Corresponding author. *E-mail address:* lamnn@nuce.edu.vn (Lam, N. N.)

a new cement with $C_{12}A_7$ ($12\,CaO \cdot 7\,Al_2O_3$) as a major mineral compound, has been developed. Increasing the amount of the $C_{12}A_7$ phase of the CAC is another way to accelerate the hydration rate since this phase is more active than CA and contributes greatly to the setting time of the cement. Too much of this phase can cause flash setting in the mortar and concrete, however, its percentage is typically regulated in the manufacturing process. A new blended cement systems incorporating both CAC and calcium sulfate ($C\$H_x$) have been developed to utilize the rapid hardening characteristics of rich $C_{12}A_7$ CAC but at a reduced cost because of the ratio of CaO/Al_2O_3 in $C_{12}A_7$ increased closer to the one of ettringite [10–13], which leads to the quick formation of ettringite with a higher content.

The hydration of an ettringite binder containing calcium aluminate cement (CAC) and calcium sulfate ($C\$H_x$) induces ettringite ($C_6A\$_3H_{32}$) and aluminum hydroxide (AH_3) as follows [14–16]:

$$C_{12}A_7 + 12\,C\$H_x + (137-12x)\,H \longrightarrow 4\,C_6A\$_3H_{32} + 3\,AH_3 \quad (1)$$

In order to have more understandings about the hydration of ettringite binder consisting rich $C_{12}A_7$ cement, some important characteristics were investigated such as setting time, chemical shrinkage, endogenous shrinkage, porosity and pore distribution by Mercury intrusion porosimetry (MIP) and bound water by DTA-TG analysis. In addition, the relationship of these properties is also discussed.

2. Materials and test methods

2.1. Materials

The binder used in this research consists of 75% by weight of the rich $C_{12}A_7$ calcium aluminate cement and 25% by weight of hemihydrate $C\$H_{0.5}$. The amount of $C_{12}A_7$, CA, C_3A, $C_4A_3\$$, C_2S and Ferrite in CAC was 57.2%, 2.1%, 0.4%, 0.3% and 18.1% by weight, respectively, which were determined by the Rietveld quantitative phase analysis. This binder has a water/binder ratio of 0.3.

2.2. Test methods

After mixing, the Vicat penetration according to EN 196-3 and chemical shrinkage as per ASTM C1608 of the pastes were determined.

The endogenous shrinkage of the paste was measured as described in detail in [17]. A rubber membrane containing binder paste was submerged in water. The change of volume of the cement paste was measured by the amount of liquid displaced by the immersed sample, typically by measuring its weight change. This method is also referred as the buoyancy method.

The binder paste was cast in small closed plastic bottles. After being cured for 2h, 3h, 5h, 10h, 24h, the solid binder then was crushed and immediately immersed in the acetone solution in further two days to stop hydration. After that, the pieces of samples with a size of about 1 cm^3 were placed in a desiccator to remove the acetone and ensure that no further hydration could be taken place. The specimens then were used for pore structure analysis or bound water analysis.

The pore structure of specimens was determined by mercury intrusion porosimetry. This measurement was performed with the Micromeritics Auto Pore IV. The specimen was placed in a glass tube and filled with a non-wetting liquid (mercury) under vacuum conditions with a pressure of less than 50 μm/Hg. The glass tube with the specimen and mercury was subsequently placed in a high-pressure analysis port. The high-pressure analysis port utilized oil to continue pressing mercury into the specimen, with a pressure ranging from 14.7 psi to 60,000 psi, and the intrusion mercury volume was recorded at each pressure point.

The hardened binders were also ground into small powder (< 50 μm) to determine the bound water in binder by heating samples to 1000˚C at a heating rate of 10˚C/min. The content of bound water in binder was calculated based on the weight of samples at 30˚C and 300˚C as presented in the Fig. 1:

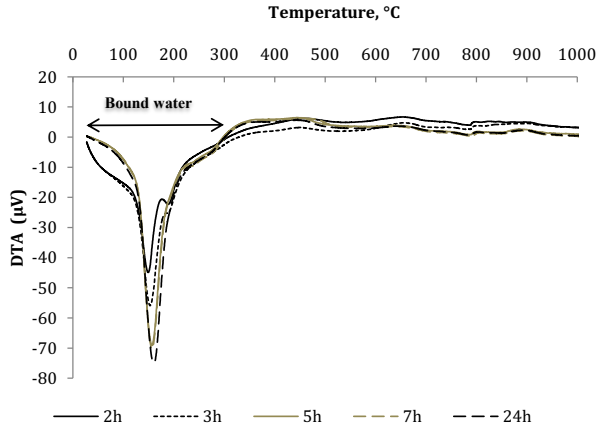


Figure 1. Calculation scheme of bound water in binder

3. Results and discussion

3.1. Vicat penetration of paste with time

The setting time presented by the Vicat penetration is an indicator presenting the liquid - solid transition, which is very important in assessing practical construction operations, such as finishing, sawcutting and curing, etc... The results of Vicat penetration with time of the binder consisting of 75% rich $C_{12}A_7$ cement and 25% hemihydrate are shown the Table 1.

Table 1. Setting time of ettringite binder paste

Time (minutes)	Vicat penetration (mm)	Time (minutes)	Vicat penetration (mm)
0	40	42	25
5	40	43	22
10	40	44	20
15	40	45	19
20	40	46	17
25	40	47	13
30	40	48	9
35	40	49	6
38	39	50	3
39	36	51	1
40	33	52	0.5
41	29	53	0.5

The research results showed that after 38 minutes of hydration, the setting process of paste was started. At this moment, the hydration products, especially ettringite and AH_3, were generated more

and more and begin to create a skeleton structure in the paste. With progress of hydration process, hydration products were crystallized and enlarged, and this leads to the liquid-solid transition process.

3.2. Chemical shrinkage, autogenous shrinkage

The correlation between autogenous shrinkage and chemical shrinkage during the early ages is depicted in Fig. 2. Overall, it is observed that this relationship is not linear to chemical shrinkage, and that no simple relationship exists between them. It is caused by the change of the macroscopic volume that occurs concurrently with chemical shrinkage, can be observed either expansively or contractively. The expansion of ettringite binder paste is due to the formation of ettringite but this shrinkage reaction is accompanied by chemical shrinkage.

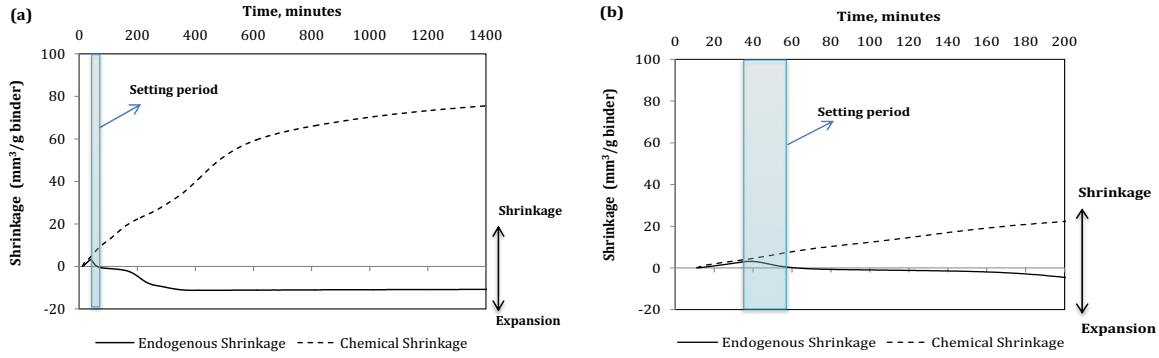


Figure 2. Chemical shrinkage and endogenous shrinkage of binder
a) During the first 24h (1400 minutes); b) During the first 200 minutes

In the first stage before initial setting time, about 40 minutes of hydration, the binder is very fluid and all volume change of binder paste is attributed to chemical shrinkage. It should be noted that the liquid stage the binder paste with high plasticity does not cause any stress in the paste. In Fig. 2, the autogenous shrinkage curve is coinciding with the chemical shrinkage as long as there is insufficient binder stiffness to resist the forces. This means that autogenous shrinkage is nearly equal to chemical shrinkage for a short period before the initial setting time. In the next stage, at about 53 minutes after hydration, the binder paste begins to stiffen and forms an initial skeleton, while the continuing chemical shrinkage stresses induce a strain in the binder as autogenous shrinkage. The binder begins to expand after the initial setting time, but expansion rate will not increase any more after 300 minutes (5 hours) of hydration. This proves that the binder after 5h has sufficiently strength to resist the expansion stress caused by ettringite formation.

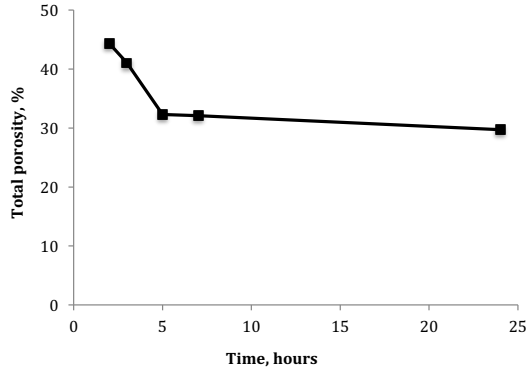


Figure 3. Total porosity of binder with time

3.3. Pore distribution

The experimental results of the specimens were determined by MIP methods and were shown in the Figs. 3–5. Fig. 3 shows the total porosity and Figs. 4–5 present the relationship between mercury

intrusions and pore sizes.

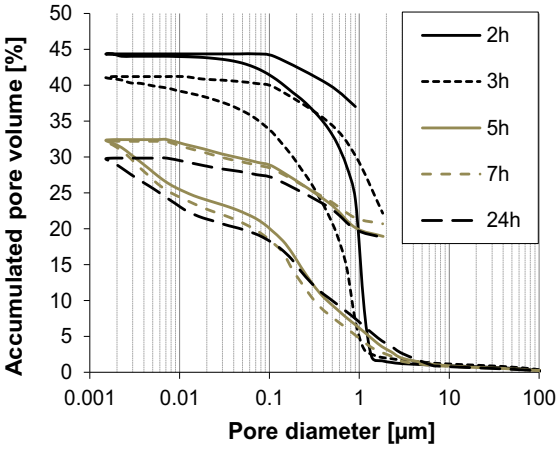


Figure 4. Accumulated pore volume of hardened binder for different curing time

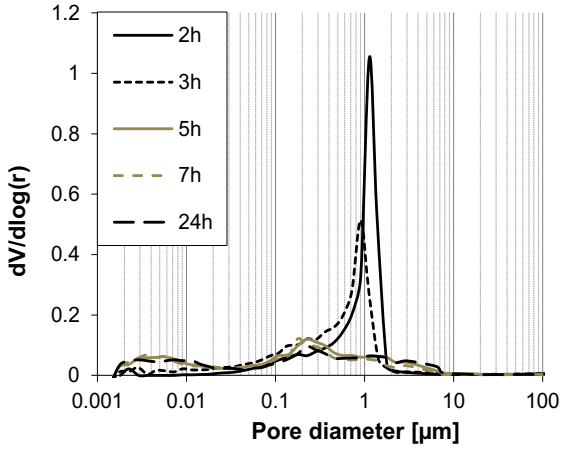


Figure 5. Pore size distribution of hardened binder for different curing time

The results in the Fig. 5 show that total pore volume of samples decreased at different curing time, from 44.34% at 2h to 32.32% at 5h, but with a slight decrease from 5h to 24h due to the rapid hydration rate of CAC and hemihydrate. In Figs. 4 and 5, it is easily observed that both capillary pore ($> 0.01\ \mu$m) and gel pore ($< 0.01\ \mu$m) increased significantly during the first 5 hours of hydration and that most pore diameters of the specimens are distributed between 0.01 μm to 2 μm.

The pore size distribution differential curve is obtained by taking the slope of the pore size distribution curve the Log Differential Intrusion against pore sizes in Fig. 5. The peaks in Fig. 5 represent the pore diameters corresponding to the higher rate of mercury intrusion per change in pressure. These peaks are called "threshold" pore diameters. The peak at around 1 μm could be found on the curve of sample at 2h and 3h and more finer peak (around 0.2 μm) at later age. This may be caused by the enlargement of gel pore due to the hydration evolution.

3.4. Bound water in hardened binder

The evolution of bound water in hardened binder determined by DTA-TG method is shown in Fig. 6 and the total porosity as a function of bound water is shown in Fig. 7.

It can be observed that the amount of bound water increases rapidly from 2h to 5h due to the rapid hydration of the binder and then decreased. The binder also exhibits the same behavior as porosity characteristic. This is not surprising since the binders are dominated by rapid formation of ettringite. This further implies that bound water can represent the hydration of ettringite binder at early age. It is confirmed by comparing bound water with porosity of hardened binder paste in the Fig. 7.

The results of the bound water versus its porosity in Fig. 7 show a linear relation. Any interpolation point at porosity can find the value of bound water. This comes with no surprise since the hydration products, which are proportional to bound water, form the more and more and fill into the pores and decreases the total porosity of system.

4. Conclusions

From the tested results of the microstructure properties of quick hardening binder based on rich $C_{12}A_7$ calcium aluminate cement, some conclusions can be withdrawn as below:

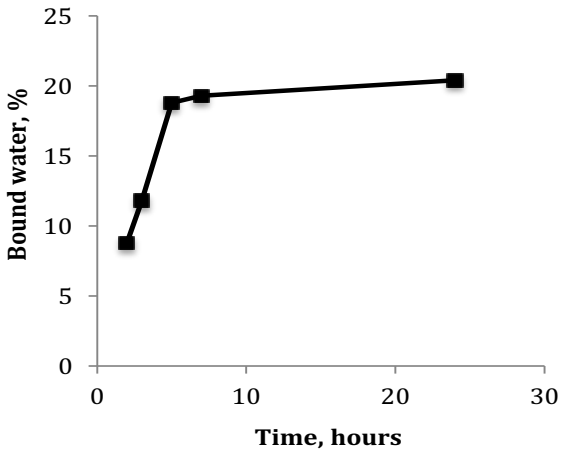


Figure 6. Evolution of bound water in binder with time

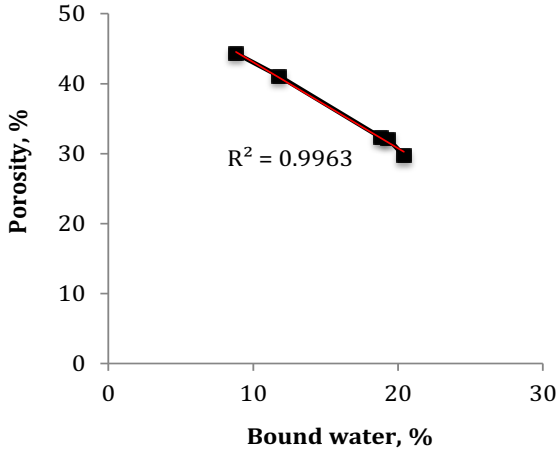


Figure 7. Relation between total porosity and bound water

- The setting time of binder containing the rich $C_{12}A_7$ calcium aluminate cement and hemihydrate takes place earlier when compared to that of OPC or standard CAC, only 40–50 minutes after mixing with water.

- The binder paste begins to expand rapidly just after the initial setting time. This expansion period prolongs until 5h of hydration.

- The porosity and bound water varied dramatically during the first 5 hours of hydration. There is also a good correlation between bound water and porosity and these two parameters showed the same development at early-age.

References

[1] World Bank (2016). *Vietnam 2016: Rapid flood damage and needs assessment*. World Bank report.

[2] Texas Department of Transportation (2004). *Standard specifications for construction and maintenance of highways, streets, and bridges*.

[3] Bizzozero, J. and Scrivener, K. L. (2014). Hydration and microstructure of rapid-strength binders based on OPC accelerated by early ettringite formation. In *Proceedings of the International Conference on Calcium Aluminates*, Avignon, France.

[4] Fryda, H., Berger, S., Bordet, F., Andreani, P. A., Martinet, A., and Brigandat, P. (2014). Ultra fast hydration opening new application fields: a comparison of different calcium aluminate technologies. In *Proceedings of the International Conference on Calcium Aluminates*, Avignon, France.

[5] Onishi, K. and Bier, T. A. (2010). Investigation into relations among technological properties, hydration kinetics and early age hydration of self-leveling underlayments. *Cement and Concrete Research*, 40(7): 1034–1040.

[6] Le Bihan, T. (2010). Etude du comportement des chapes autonivelantes en ciment sulfo-alumineux: outils expérimentaux et de modélisation. PhD thesis, INSA Lyon, 2010, in French.

[7] Klaus, S. R., Neubauer, J., and Goetz-Neunhoeffer, F. (2013). Hydration kinetics of CA2 and CA–investigations performed on a synthetic calcium aluminate cement. *Cement and Concrete Research*, 43: 62–69.

[8] Damidot, D., Rettel, A., and Capmas, A. (1996). Action of admixtures on fondu cement: Part 1. Lithium and sodium salts compared. *Advances in Cement Research*, 8(31):111–119.

[9] Damidot, D., Rettel, A., Sorrentino, D., and Capmas, A. (1997). Action of admixtures on fondu cement:

II. Effect of lithium salts on the anomalous setting time observed for temperatures ranging from 18 to 35°C. *Advances in Cement Research*, 9(35):127–134.

[10] Martin, I., Patapy, C., and Cyr, M. (2014). Parametric study of binary and ternary ettringite-based systems. In *Proceedings of the International Conference on Calcium Aluminates*, Avignon, France.

[11] Scrivener, K. L. and Capmas, A. (1998). *LEA's Chemistry of Cement and Concrete*, chapter 13: Calcium Aluminate Cements. Elsevier Science & Technology Books - London.

[12] Le Saout, G., Lothenbach, B., Taquet, P., Fryda, H., and Winnefeld, F. (2014). Hydration study of a calcium aluminate cement blended with anhydrite. In *Proceedings of the International Conference on Calcium Aluminates*, Avignon, France.

[13] Andreani, P. and Touzo, B. (2014). Mineral composition and hydration of a $C_{12}A_7$ rich binder. In *Proceedings of the International Conference on Calcium Aluminates*, Avignon, France.

[14] Lamberet, S. (2005). Durability of ternary binders based on Portland cement, calcium aluminate cement and calcium sulfate. PhD thesis, Ecole Polytechnique Federale de Lausanne, Switzerland.

[15] Georgin, J. F. and Prud'homme, E. (2015). Hydration modelling of an ettringite-based binder. *Cement and Concrete Research*, 76:51–61.

[16] Bayoux, J., Bonin, A., Marcdargent, S., Verschaeve, M., and Mangabhai, R. J. (1990). *Study of the hydration properties of aluminous cement and calcium sulphate mixes*. Calcium aluminate cements - E. & F. N. Spon, Chapman & Hall, London.

[17] Lura, P. and Jensen, O. M. (2007). Measuring techniques for autogenous strain of cement paste. *Materials and Structures*, 40(4):431–440.